

Description of magnetic moments within the Gogny Hartree-Fock-Bogolyubov framework: Application to Hg isotopes

S. Péru^{1,2}, S. Hilaire^{1,2}, S. Goriely³ and M. Martini^{4,5}

¹CEA, DAM, DIF, F-91297 Arpaçon, France

²Université Paris-Saclay, CEA, LMCE, 91680 Bruyères-le-Châtel, France

³Institut d'Astronomie et d'Astrophysique, Université Libre de Bruxelles, Campus de la Plaine, CP-226, 1050 Brussels, Belgium

⁴IPSA-DRII, 63 boulevard de Brandebourg, 94200 Ivry-sur-Seine, France

⁵Sorbonne Université, Université Paris Diderot, CNRS/IN2P3,

Laboratoire de Physique Nucléaire et de Hautes Energies (LPNHE), Paris, France



(Received 21 April 2021; accepted 2 August 2021; published 25 August 2021)

While the ground state configuration is classically determined by the variational principle minimizing the binding energy of the system, we propose here a different procedure to identify the configuration of the ground state in odd- A nuclei. This procedure is based on the Hartree-Fock-Bogolyubov (HFB) framework with a self-consistent blocking of the unpaired nucleon and identifies the ground state as the blocked quasiparticle configuration compatible with the observed spin and parity and, most importantly, the measured magnetic moment. The magnetic moments are calculated within the HFB framework for all odd Hg isotopes for which experimental data is available. To validate the method, a systematic comparison between the predicted and measured electric quadrupole moments and isotopic shifts is performed. For even-even isotopes, we show that the ground state deformation, and more particularly the competition between the prolate and oblate shapes, can hardly be determined through a comparison of the QRPA β -decay half-life with experiment, though this approach also calls for an observable similar to the one used for odd- A isotopes, namely the spin-flip component of the isovector part of the magnetic moment operator. For even isotopes with shape coexistence, no adequate constraint could be identified, except though the charge radius. Assuming light even-even Hg isotopes to have an oblate shape, the resulting charge radii staggering observed in the Hg chain by laser spectroscopy can through this identification procedure be reproduced.

DOI: [10.1103/PhysRevC.104.024328](https://doi.org/10.1103/PhysRevC.104.024328)

I. INTRODUCTION

The radioactive isotopes in the neutron-deficient lead region have been studied by optical spectroscopy for several decades due to the extraordinary measurements of the so-called staggered pattern found experimentally in particular within the Hg isotopic chain region [1]. In particular, $^{181,183,185}\text{Hg}$ present a charge radius significantly larger than their even-even neighbours, in contrast to what is observed for heavier Hg isotopes. This important discovery of shape staggering between odd and even neutron-deficient mercury isotopes is specific to this region of the nuclear chart and has been contributing significantly to our understanding of shape coexistence at low excitation energy [2–6]. This staggering is explained through different distributions of proton and neutron pairs with respect to their Fermi energies found in neighboring isotopes and isotones, leading to sudden modifications of their ground state (GS) properties.

The GS configuration within the mean-field approach is classically obtained assuming the variational principle, i.e., the GS is defined by the absolute minimum of the energy surface in the deformation plane. While this procedure is rather robust for quasispherical or well-deformed even-even nuclei,

for systems with an odd number of nucleons, it often fails to provide the right spectroscopic properties of the GS, essentially the spin and parity, hence all associated observables. In addition, for many systems, corrections beyond mean field are known to affect the energy balance between the various minima in the deformation plane [7–10]. We propose here a new procedure that identifies the GS of odd- A and odd-odd nuclei on the basis of their measured magnetic moment with the correct spin and parity. To validate the procedure, we also calculate additional observables such as the β -decay half-life, the charge radius or the electric quadrupole moment and compare them with experimental data. In such an approach, the magnetic moment plays a key role in the identification of the quantum number associated with the GS.

Nuclear moments have been studied theoretically and experimentally since the very beginning of nuclear structure physics [11]. The first measurements of nuclear magnetic moments were performed in the 1950s by the nuclear magnetic resonance technique and are routinely done nowadays by laser spectroscopy [1, 12, 13]. A comprehensive compilation of magnetic moments measured up to 2004 can be found in Ref. [14]. From the theory side, the magnetic dipole response can be successfully described within the quasiparticle random

phase approximation (QRPA) approach [15–17]. Here we propose to estimate an effective magnetic moment operator with respect to the approximation made by the Hartree-Fock-Bogoliubov (HFB) method. Our theoretical framework is described in Sec. II. In Sec. III, the identification of the GS of even- and odd- A Hg isotopes is discussed. For odd Hg isotopes (Sec. III A), the GS configuration is identified by comparing the calculated magnetic moment of the various potential states with experiment. In contrast, for even-even Hg isotopes (Sec. III B), where no similar quantities can be obtained, another protocol related to the β -decay half-life is explored.

In Sec. IV, the charge radius and electric quadrupole moment of the identified GS of the Hg isotopes are estimated and compared with measured values. Conclusions and perspectives are finally given in Sec. V.

II. THEORETICAL FRAMEWORK

The HFB formalism is well known to provide a reliable description of the GS properties of even-even systems, but also a starting point to improve the description of GS properties for systems with an odd number of nucleons or to explain excited states through approaches such as the generator coordinate method or the random phase approximation (e.g., Refs. [18,19]). At static mean-field level, the solutions of the HFB equations are quasiparticle (qp) orbitals, which set a so-called vacuum corresponding to a $J^\pi = 0^+$ state. The HFB GS of even-even nuclei is determined by minimizing the binding energy over the entire potential energy surface in the deformation plane. To describe fermion systems, such as nuclei with an odd number of nucleons, the GS should be redefined as the excitation of one qp state on top of an HFB vacuum. In practice, the qp excitation that minimizes the total energy is selected. In the present axially symmetric HFB framework, the projection K of the total angular momentum J and the parity π are good quantum numbers. Thus, the HFB GS for odd nuclei with spin-parity J^π is described by selecting a qp orbital with $K_{qp}^\pi = J^\pi$ and imposing its occupation probability. This so-called blocking approximation can be limited to the equal filling one where time-reversal symmetry is conserved. This symmetry conservation has no consequence in the present study. After variation, only one of the two qp of the blocked pair is considered as an excitation on top of the HFB vacuum to calculate observables within time breaking assessment. Among them, the spectroscopic magnetic moment is of particular interest since it contains, for fermion systems, detailed structure information in contrast to the spectroscopic quadrupole moment, which can cancel out for spin values of $J = 0$ or $1/2$.

The magnetic moment operator is known to be composed of two contributions, namely a pure spinor part and an orbital angular part [20], i.e.,

$$\hat{\mu} = g_s \hat{s} + g_l \hat{l}, \quad (1)$$

where g_s and g_l are the gyromagnetic factors. For protons $g_l = 1$, $g_s = 5.586$ and for neutrons $g_l = 0$, $g_s = -3.826$. For spherical and quasispherical nuclei (i.e., for nuclei with a quadrupole deformation parameter $|\beta| \lesssim 0.07$), the spectro-

scopic magnetic moment μ_S is equal to the intrinsic one. However, for axially deformed nuclei, μ_S can be derived from the expression

$$\mu_S = \frac{K}{J+1} \langle K | \hat{\mu} | K \rangle + G_R, \quad (2)$$

where the additional collective contribution G_R needs to be considered for well-deformed nuclei (β typically larger than 0.2). This rotational component G_R is related to the angular momentum J and can be approximated by the simple expression [21–24]

$$G_R = \frac{Z}{A} \frac{J(J+1) - K^2}{J+1}. \quad (3)$$

It is known to amount to about 0.25 for odd neutrons and 0.40 for odd protons [21]. Future work will consider a more microscopic determination of G_R within the Inglis-Belyaev approximation [24,25].

For $J = 1/2$ states, a special attention should be paid to the coupling with the $K = -1/2$ time-reversal configuration [20,22], which brings an additional contribution to the spectroscopic magnetic moment. The resulting spectroscopic magnetic moment is given by

$$\mu_S^{J=1/2} = \frac{1}{3} \left(\left\langle \frac{1}{2} \left| \hat{\mu} \right| \frac{1}{2} \right\rangle - \sqrt{2} \left\langle -\frac{1}{2} \left| \hat{\mu} \right| \frac{1}{2} \right\rangle \right) + G_R. \quad (4)$$

Finally, to introduce in an effective way beyond-mean-field and core polarization effects, the g_s gyromagnetic factor is usually reduced by a factor of 0.6–0.9 [21–23,25,26]. We adopt here a spin quenching factor of 0.75, as proposed in Ref. [26], with an uncertainty of about ± 0.15 , as studied in Ref. [25]. In the present study, two spectroscopic values for magnetic moment are consequently distinguished: the bare one μ_S and the effective one μ_S^{eff} obtained with the effective operator:

$$\hat{\mu}_{\text{eff}} = 0.75 \times g_s \hat{s} + g_l \hat{l}. \quad (5)$$

The relevance of the effective operator within the HFB framework is discussed below.

III. IDENTIFICATION OF THE GS IN HG ISOTOPES

A. Odd Hg isotopes

To test the HFB prediction of the magnetic moment, we consider the Hg isotopic chain extensively studied through recent laser spectroscopy measurements at CERN-ISOLDE radioactive ion beam facility [1,12]. In axially symmetric deformed calculations, GS shapes are traditionally determined by minimizing the potential energy curves obtained within the constrained HFB model for various quadrupole deformations. While for even isotopes only one $J^\pi = 0^+$ energy surface needs to be calculated, for odd- A nuclei, all possible qp candidates for a given spin and parity need to be blocked in the HFB calculations leading to a significant number of potential energy curves. Note that all calculations have been performed with the DIM interaction [27] and a 19 major oscillator shell basis, except for the potential energy surfaces illustrated in Fig. 1, which have been obtained with a 15 major oscillator shell basis.

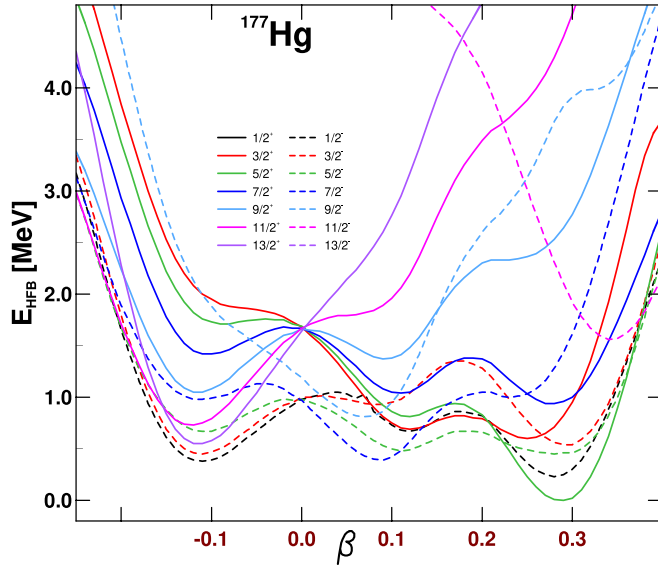


FIG. 1. ^{177}Hg axial potential energy curves for different K^π blockings as a function of the quadrupole deformation parameter β . Calculations are performed with the DIM interaction and a 15 major oscillator shell basis.

We start by focusing on the assignment of spin and parity of odd Hg isotopes. Within our axially symmetric framework, it is reasonable to propose a GS spin J corresponding to $J = K$. For odd- A , isotopes, a potential energy curve can be obtained for each value of K^π corresponding to the blocking of the odd neutron. As an example, Fig. 1 illustrates the ^{177}Hg binding energies as a function of the axial deformation parameter β for various K^π projections. Each curve is obtained by blocking self-consistently in the iterative HFB resolution the first qp state for the given K^π quantum number.

Usually, the HFB GS is described by the lowest energy configuration, i.e., the absolute minimum. As seen in Fig. 1, such a blocking method applied to DIM-HFB predicts a $J^\pi = 5/2^+$ GS in disagreement with the $7/2^-$ value suggested by experiment [28]. Other configurations having binding energies close to the absolute minimum are still candidates since beyond-mean-field correlations could modify the energy sequence without altering their respective structure properties. For well-deformed shapes ($|\beta| > 0.2$) the difference between the estimated rotational energy of both minima is $\lesssim 100$ keV and this mechanism is consequently inefficient to restore the energy sequence. To reproduce the experimental scheme, other contributions need to be explored. It should also be noticed that the binding energy difference between the HFB absolute minimum and the lowest $7/2^-$ configuration is of the order of 0.5 MeV. This difference is of the same order of magnitude as the root-mean-square deviation of the DIM mass predictions with respect to all 2408 known masses for $Z, N \geq 8$ nuclei, i.e., of the order of 0.8 MeV [27]. For this reason, all configurations with a binding energy within typically 1 MeV above the absolute minimum may reasonably be considered as potential candidates for the GS.

To identify the GS characteristics, and in particular its quantum numbers, we propose a new procedure based on the

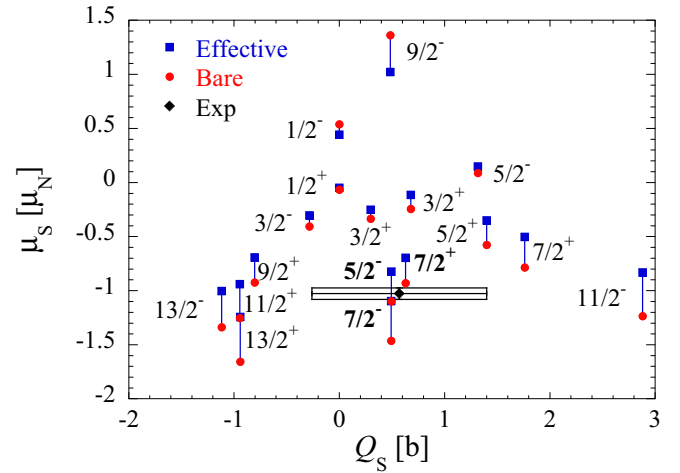


FIG. 2. D1M-HFB magnetic moments as a function of the spectroscopic quadrupole moment for the different energy minima for each K^π state shown in Fig. 1 for ^{177}Hg . The red circles correspond to the bare magnetic moments and the blue squares to the effective ones. Both are joined by a solid line for the same K^π blocked state. The bare magnetic moment for the $J^\pi = 5/2^-$ and the effective magnetic moment for the $J^\pi = 7/2^-$ are compatible with the experimental data shown by the black diamond [1,14]. For the $3/2^+$, $5/2^-$, and $7/2^+$, the moments for the second minima observed in Fig. 1 are also shown.

theoretical description of the experimental spectroscopic magnetic moment. Figure 2 shows theoretical spectroscopic magnetic moments with respect to the spectroscopic quadrupole moment for all blocked HFB minima. Both the bare and effective magnetic moments are shown and joined by a solid line. The experimental data for the assigned $7/2^-$ GS is also shown for comparison [1].

From Fig. 2, it appears that both the bare and effective operators can provide an HFB blocking configuration for which the spectroscopic magnetic and electric moments are compatible with experimental data. The corresponding GS candidates are characterized by different spins and parities, namely $K^\pi = 7/2^-$ using the effective magnetic moment and $K^\pi = 5/2^-$, or potentially $7/2^+$, if we adopt the bare magnetic moment. In contrast the $K^\pi = 5/2^+$ HFB absolute minimum is seen to be incompatible with both the measured magnetic and electric moments. Since the experimentally suggested GS is a $7/2^-$ state, this example clearly illustrates the relevance of considering the effective magnetic moment operator and not the bare one. The HFB GS is neither given by the configuration leading to the lowest absolute energy, nor by the blocked states with a bare magnetic moment compatible with experiment. However, considering the effective magnetic moment, all data are found to be compatible with the $K^\pi = 7/2^-$ blocked configuration.

The three above-mentioned HFB blocking candidates can also be tested on the charge radius recently measured and giving rise to an isotopic shift with respect to ^{198}Hg of $\delta \langle r^2 \rangle_{\text{exp}}^{A-198} = -1.067(8)\{78\} \text{ fm}^2$ [1]. We find for our three candidates $K^\pi = 7/2^-$, $5/2^-$, and $7/2^+$, an isotopic shift of $\delta \langle r^2 \rangle^{A-198} = -1.33$, -1.28 , and -1.29 fm^2 , respectively,

while for the $5/2^+$ HFB absolute minimum, $\delta\langle r^2 \rangle^{A-198} = -0.57 \text{ fm}^2$. The latter is clearly incompatible with experimental data. A more detailed comparison with charge radii is presented in Sec. IV.

The above-described protocol for identifying the GS can similarly be applied to the other Hg isotopes. For ^{179}Hg , the HFB $J^\pi = K^\pi = 1/2^-$ configuration found as the absolute minimum does not match the experimental tentative assignment $J^\pi = (7/2^-)$. Only the $7/2^-$ configuration close to a spherical shape appears to be compatible with experiment. Its HFB spectroscopic moments are estimated to $\mu_S^{\text{eff}} = -1.11\mu_N$ and $Q_S = 0.58 \text{ b}$ in rather good agreement with measured value of $\mu_S^{\text{exp}} = -0.949(29)\mu_N$ and $Q_S^{\text{exp}} = 0.77(28) \text{ b}$.

For both ^{181}Hg and ^{183}Hg isotopes, we only found one compatible candidate with $J^\pi = K^\pi = 1/2^-$, as determined experimentally. The effective spectroscopic magnetic moments [calculated from Eq. (4)] are $\mu_S^{\text{eff}} = 0.48\mu_N$ for ^{181}Hg and $\mu_S^{\text{eff}} = 0.45\mu_N$ for ^{183}Hg , in rather good agreement with experimental data $\mu_S^{\text{exp}} = 0.510(9)$ and $0.516(11)\mu_N$, respectively. On top of that, the intrinsic deformation of these blocking HFB configurations is found to be prolate with $\beta = 0.31$ for ^{181}Hg and 0.29 for ^{183}Hg in agreement with the interpretation made by the shell model calculations [1]. Note that for these Hg isotopes, the same assignment is obtained with the effective or bare magnetic moment.

When dealing with the ^{185}Hg GS, a more complex situation is found. In particular, none of the calculated magnetic moments obtained by blocking the first K^π qp states with a reasonably low binding energy coincides with the experimental value $\mu_S^{\text{exp}} = 0.509(4)\mu_N$ [1,12]. However, the HFB binding energy of the second $1/2^-$ blocked qp state above the $7/2^-$ minimum minimum is low enough ($\Delta E = 1.1 \text{ MeV}$) to be considered. For this blocked solution with prolate deformation ($\beta = 0.27$) the effective magnetic moment amounts to $\mu_S^{\text{eff}} = 0.43\mu_N$. It is therefore possible here again to identify the structure of the ^{185}Hg GS by constraining the magnetic moment, leading to a $J^\pi = K^\pi = 1/2^-$ state with a prolate intrinsic deformation.

Concerning ^{187}Hg , the situation becomes even more complex. Although the magnetic moment $\mu_S^{\text{eff}} = -0.68\mu_N$ of the $J^\pi = 9/2^+$ HFB absolute minimum is compatible with the experimental one associated with a $J^\pi = 3/2^-$ GS, this configuration cannot correspond to the HFB GS since its spectroscopic quadrupole moment $Q_S = 2.15 \text{ b}$ is far from the measured $Q_S^{\text{exp}} = -0.8(3) \text{ b}$. For this isotope, only the blocked $3/2^-$ qp states are found to reproduce the experimental magnetic moment. To remove this ambiguity on the HFB configuration assignment, it remains possible to consider the quadrupole moment as an additional criterion. It turns out that the only candidate fully compatible with experiment is the third blocked qp, which corresponds to an oblate $3/2^-$ state. Its HFB energy lies about 1.36 MeV above the $9/2^+$ energy minimum minimum. Similar conclusions are reached for $^{189,191,193}\text{Hg}$ isotopes, where the blocking of the $3/2^-$ qp state reproduces both the measured magnetic and electric moments. For the three isotopes, an oblate shape is predicted for the corresponding GS, as found experimentally [12].

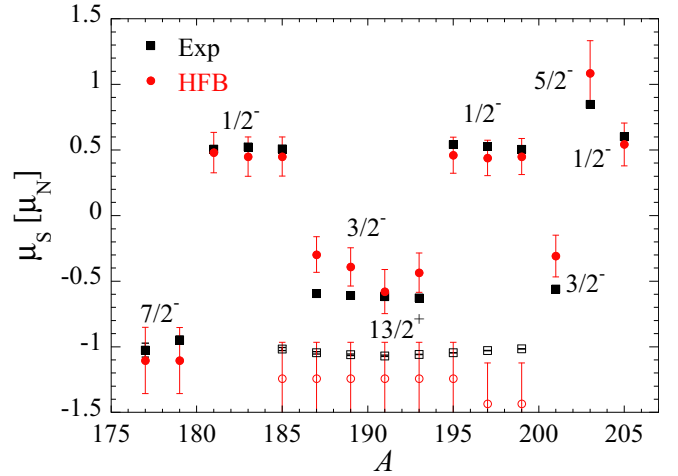


FIG. 3. Comparison between experimental [1,12,14] and HFB magnetic moments for the various Hg isotopes. The full symbols correspond to the GS and the open symbols to the isomeric states. The corresponding spins are given. Details on the theoretical error bars can be found in the text.

For $^{195,197,199}\text{Hg}$ isotopes, $J^\pi = K^\pi = 1/2^-$ configurations compatible with experiment are also found (Fig. 3). For these three specific cases, the additional component in Eq. (4) is found to increase the magnetic moment by typically $0.2 \mu_N$. The same above-described protocol to identify the qp blocking configuration as actual GS has been applied up to ^{203}Hg . Consequently, HFB calculations provide two sets of results, namely the first one based on the absolute HFB energy minima, and the second one based on the magnetic moment selection provided experimental data is available. In the latter case, an actual GS compatible with experimental spin, parity, electric, and magnetic moments can be found. Note that a similar procedure constraining the spin and parity on experimental data has been applied within the spherical relativistic Hartree-Bogolyubov framework to explain the kink in the isotopic shifts for heavier Hg isotopes around the $N = 126$ closed shell [29]. Since the corresponding magnetic moments have not been measured yet for such heaviest $A \geq 207$ isotopes, our present study is restricted to $N \leq 126$ Hg isotopes.

We compare in Fig. 3 the experimental magnetic moments for the ground states with those obtained through our HFB assignment protocol. For completeness, we also estimate the magnetic moment of the isomeric states $13/2^+$ for the $A = 185-199$ nuclei and compare them with measured values [1,12,14]. For each state, a theoretical uncertainty can be attributed. It corresponds to a quadratic sum of uncertainties associated with

- (1) the effective spin quenching factor: it is estimated to amount to 20% of the magnetic moment (see Sec. II);
- (2) the determination of the rotational correction as well as its contribution depending on the exact quadrupole deformation: it is estimated to about $\pm 0.1\mu_N$;
- (3) the interaction adopted: calculations performed with the DIS interaction give an average deviation of $\pm 0.07\mu_N$ on the GS magnetic moments with respect

TABLE I. Quadrupole deformation parameters β and binding energies of the oblate “ o ” and prolate “ p ” minima in even Hg isotopes calculated within the HFB framework using the DIM interaction [27] and assuming axial symmetry with a 19 major oscillator shell basis. For the two heaviest isotopes close to the $N = 126$ neutron shell closure, a spherical shape $\beta = 0$ is found and referred to in the oblate column.

A	β_o	E_o [MeV]	β_p	E_p [MeV]	$E_o - E_p$ [MeV]
178	-0.11	-1383.62	+0.29	-1383.84	0.22
180	-0.13	-1403.67	+0.31	-1404.28	0.61
182	-0.15	-1423.28	+0.30	-1423.94	0.66
184	-0.15	-1442.41	+0.29	-1442.84	0.45
186	-0.15	-1461.04	+0.28	-1461.05	0.01
188	-0.15	-1479.18	+0.26	-1478.31	-0.87
190	-0.14	-1496.84	+0.10	-1495.54	-1.30
192	-0.14	-1514.03	+0.09	-1512.71	-1.32
194	-0.13	-1530.74	+0.09	-1529.47	-1.27
196	-0.12	-1546.93	+0.07	-1545.82	-1.11
198	-0.11	-1562.59	+0.04	-1561.82	-0.77
200	-0.08	-1577.80	-	-	<0
202	0.00	-1592.98	-	-	<0
204	0.00	-1607.91	-	-	<0

to those obtained with DIM. For the $13/2^+$ isomeric states, similar predictions are obtained with both interactions.

The resulting uncertainties affecting the magnetic moment of the newly assigned ground and isomeric states are shown in Fig. 3.

B. Even Hg isotopes

The above-described protocol to estimate the GS configuration on the basis of the magnetic moments can obviously not be applied to even-even Hg isotopes. Even- N Hg isotopes are known to be subject to shape coexistence, as shown in Table I by the binding energies of the prolate and oblate minima for the Hg nuclides ranging between $A = 178$ and 204 estimated within the HFB framework. The last column provides the energy difference between the oblate and the prolate wells.

As expected, for the heavy $A > 186$ Hg isotopes, the prolate minimum progressively disappears, giving place to a shallow oblate minimum, which finally migrates towards sphericity close to the $N = 126$ shell closure. For the light Hg isotopes with $A = 178$ –186, the prolate and the oblate minima are relatively degenerate and should be mixed including beyond-mean-field corrections [7–10,30,31]. Nevertheless, a recent comparison between the experimental spectra and the theoretical ones obtained by the five-dimensional collective Hamiltonian (5DCH) approach including triaxial degree of freedom for ^{188}Hg [4] has shown that the predicted intrinsic deformation of the first and second 0^+ can be inverted with respect to experimental evidence. Such a discrepancy in the relative excitation energy is found although the absolute minimum of the potential energy surface is oblate as experimentally expected (see Sec. IV). Even if all rotational

and vibrational bands are properly reproduced, the 5DCH approach keeps on failing in the GS structure assignment and, in particular, supports the prolate shape over the spherical or oblate ones. On top of that, the 5DCH approach describes only positive parity states on the basis of the unique $J^\pi = 0^+$ potential energy surface, hence is limited up to now to even-even nuclei. For these reasons, this dynamical 5DCH approach may not be pertinent for improving the description of such intrinsic observables and will not be followed in the present study. At this stage, both GS candidates corresponding to the oblate and prolate HFB minima should be considered, though some alternative approaches may help us to differentiate them.

A tentative determination of the GS intrinsic deformation of even- N Hg isotopes considers the β -decay half-lives prediction. This choice is motivated first by the similarity between the isovector spin-flip component of the magnetic moment and the Gamow-Teller operator and second by the analysis of the deformation effects on β -decay patterns obtained in Ref. [32] with the Skyrme interaction for the same isotopic chain. In the present work, we plan to deduce the intrinsic GS deformation in even- N Hg isotopes through the best simultaneous description of the experimental β -decay half-lives of the even-even Hg isotopes and the GS magnetic moment of the corresponding odd-odd daughter Au isotopes.

To calculate the β -decay half-lives we follow the axially symmetric HFB+QRPA approach developed in Ref. [33] for the Gogny forces. This approach was used to estimate the β^- -decay half-lives of all the even-even nuclei for which experimental data exist as well as the exotic neutron-rich $N = 82$, 126, and 184 isotones. The Gamow-Teller response of even and odd $^{90-94}\text{Zr}$ isotopes [16] and β^- -decay of ^{83}Ga [34] have also been successfully studied within the same approach. In the same framework, β^+ and electron-capture (EC) decay rates have been estimated for ^{188}Bi [35]. In the present study, we follow the same approach and estimate the β^+ and EC decay half-lives of $^{182,184,186}\text{Hg}$ isotopes to choose between the oblate or prolate configurations. Both the allowed Fermi and Gamow-Teller transitions are included. The folding of the Gamow-Teller strengths is the same as the one employed in Ref. [33]. The allowed EC contribution is also included, as described in Ref. [36].

Turning to the identification of different possible configurations for the GS of the daughter $^{182-186}\text{Au}$ isotopes, we adopt the same protocol as described in Sec. III A. However, since the considered Au isotopes are odd-odd nuclei and the underlying HFB calculation does not break time-reversal symmetry, the calculation of magnetic moment may be affected by a larger uncertainty with respect to the odd-even cases previously discussed. Furthermore, since configurations with either a proton up plus neutron up or a proton up plus neutron down remain degenerate in the present approach, the corresponding excitation energies should be taken with caution. For this reason, a larger tolerance is considered to identify the configurations compatible with the GS assignment. It is important also to emphasize that HFB calculations of odd-odd nuclei were already performed in the context of our β -decay study for even-even nuclei [33] in order to obtain the β strengths as a function of the excitation energy of the daughter odd-odd nucleus. The procedure to evaluate the reference energy in

the odd-odd nucleus is explained in detail in Ref. [33]. The method introduced here represents an improvement of that procedure.

Concerning the $^{182}\text{Hg} \rightarrow ^{182}\text{Au}$ decay, two ^{182}Au HFB minima are compatible with the experimental assignments of $J^\pi = 2^+$ and $\mu_S^{\text{exp}} = 1.30(10)\mu_N$ [14]: these correspond to the same $(\pi 3/2^- \uparrow, \nu 1/2^- \uparrow)$ configurations with $\mu_S^{\text{eff}} = 1.40\mu_N$, $\beta = 0.29$, $\Delta E = 0.72$ MeV or $\mu_S^{\text{eff}} = 1.33\mu_N$, $\beta = -0.16$, $\Delta E = 1.63$ MeV (where ΔE is the HFB excitation energy with respect to the absolute minimum). This configuration assignment in ^{182}Au is in agreement with recent experimental analysis [37]. These daughter nucleus configurations, irrespective of the shape, provide a different reference energy value in the mother nucleus, hence a different prediction of the β -decay rate. More specifically, the $\beta^+ + \text{EC}$ ^{182}Hg half-life is estimated to $T_{1/2}^{\text{QRPA}} = 7.8$ s and 14.4 s for the ^{182}Hg GS oblate and prolate shapes, respectively. When compared to $T_{1/2}^{\text{exp}} = 10.83$ s [38], none of these GS shapes can be clearly excluded.

In the case of $^{184}\text{Hg} \rightarrow ^{184}\text{Au}$ decay, the $(\pi 3/2^- \uparrow, \nu 7/2^- \uparrow)$ ^{184}Au GS configuration leads to an HFB magnetic moment $\mu_S^{\text{eff}} = 2.10\mu_N$ in agreement with experimental GS assignments of $J^\pi = 5^+$ and $\mu_S^{\text{exp}} = 2.07(2)\mu_N$ [14,39]. Within this assignment, we find a β -decay half-life $T_{1/2}^{\text{QRPA}} = 120$ s for the mother oblate shape and 56 s for the prolate one. Both theoretical half-lives are in disagreement with the experimental $T_{1/2}^{\text{exp}} = 30.87$ s [38]. Finally, for $^{186}\text{Hg} \rightarrow ^{186}\text{Au}$, we found two prolate ^{186}Au HFB minima compatible with the experimental assignments of $J^\pi = 3^-$ and $\mu_S^{\text{exp}} = -1.28(3)\mu_N$ [14], i.e., the $(\pi 3/2^- \downarrow, \nu 9/2^+ \uparrow)$ configuration with $\beta = 0.28$, $\mu_S^{\text{eff}} = -1.35\mu_N$ and the $(\pi 1/2^- \downarrow, \nu 7/2^+ \uparrow)$ one with $\beta = 0.27$, $\mu_S^{\text{eff}} = -1.43\mu_N$. The corresponding QRPA half-lives are $T_{1/2}^{\text{QRPA}} = 377$ s and 410 s for the prolate ^{186}Hg minimum and 286 s and 136 s for the oblate one. Both overestimate the experimental value $T_{1/2}^{\text{exp}} = 82.3$ s [40].

In summary, the β -decay half-life cannot be determined accurately enough at the present time by the QRPA approach to constrain the intrinsic GS deformation in the mother nucleus. This complex situation found for even-even nuclei also illustrates the relevance of considering the magnetic moment to identify the GS in odd- A or odd-odd nuclei.

IV. ISOTOPIC SHIFT AND SPECTROSCOPIC QUADRUPOLE MOMENTS

With the GS configuration of the odd Hg isotopes identified, as described in Sec. III A, we compare in Fig. 4 the HFB isotopic shifts with experimental data for the GS of all Hg isotopes. As discussed in Sec. III B, for the light even isotopes with $A = 178$ – 186 , it has not been possible to distinguish between the oblate or prolate intrinsic configurations. For this reason, we show in Fig. 4 both theoretical predictions. It clearly appears that the measurement of isotopic shift favors the oblate configuration for the even $^{178-186}\text{Hg}$ isotopes. Only with such an assumption, it is possible to reproduce the staggering observed for the GS of $180 \leq A \leq 186$ nuclides.

Some deviations can also be observed for the lightest isotopes, where the charge radii are seen to be underestimated

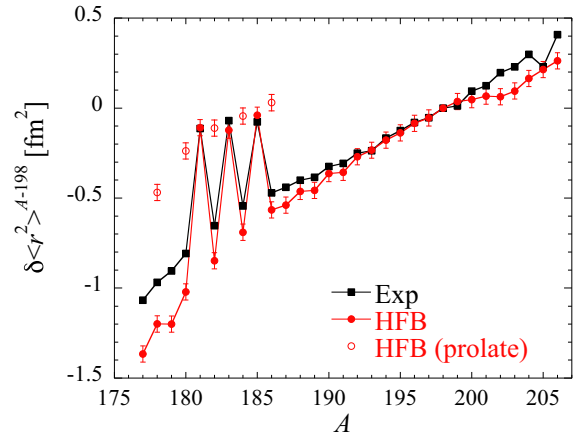


FIG. 4. Comparison between experimental [1,12] and HFB isotopic shifts $\delta \langle r^2 \rangle^{A-198}$ for the various Hg isotopes. For the even $A = 178$ – 186 isotopes, the isotopic shift for the prolate HFB configurations are shown with open circles. The corresponding full circles for even $A = 178$ – 186 correspond to the oblate configuration.

with respect to the experimental ones. Beyond static mean-field calculation may induce some dynamical deformation, which could increase the charge radii for isotopes with a relatively soft quadrupole deformation.

A comparison with DIS predictions shows that on average a systematic deviation of 0.045 fm^2 can affect $\delta \langle r^2 \rangle^{A-198}$. Such an uncertainty is illustrated by the theoretical error bars in Fig. 4.

A similar comparison can be made for the electric quadrupole moments. In the present study, the quadrupole moment is estimated from the proton and not the charge distribution. The impact of the charge distribution will be estimated in a forthcoming study. The experimental and calculated moments are compared in Fig. 5. The agreement is found to be rather satisfactory. A systematic uncertainty of 0.055 b is shown on $J > 1/2$ predictions, corresponding to

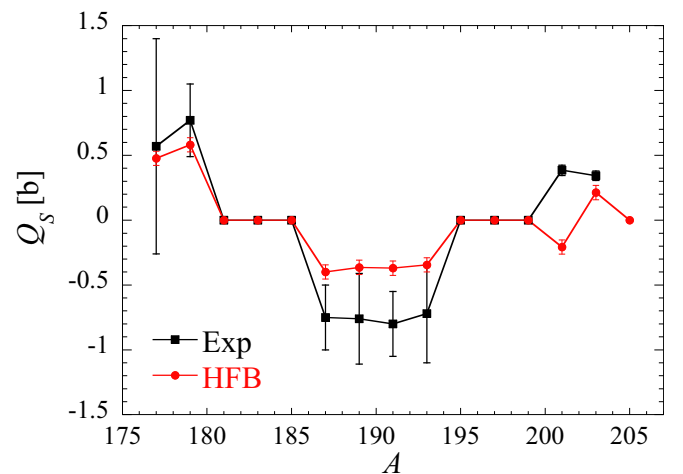


FIG. 5. Comparison between experimental [12,14] and HFB spectroscopic quadrupole moments for the odd- N Hg isotopes.

the average deviation obtained between calculations using the D1S or D1M interactions.

V. CONCLUSION AND PERSPECTIVES

While the GS configuration is classically determined by the variational principle minimizing the binding energy of the system, in the present study, we propose a different procedure to identify the GS configuration and applied it to the Hg isotopic chain. For odd-*A* isotopes, this procedure is based on the HFB calculation with a self-consistent blocking of the unpaired nucleon and the identification of the GS configuration as the blocked qp compatible with the observed spin and parity and, most importantly, the measured magnetic moment. For even-even isotopes, the GS deformation, and more particularly the competition between the prolate and oblate shapes, could not be determined through a comparison of the QRPA β -decay half-life with experiment, though this approach also calls for an observable similar to the one used for odd-*A* isotopes, namely the spin-flip component of the isovector part of the magnetic moment operator, even when identifying the GS configuration of the daughter nucleus through its magnetic moment.

The magnetic moments have been calculated within the HFB framework for all odd Hg isotopes for which experimental data is available. The corresponding configurations have been used to estimate the electric quadrupole

moment and charge radii that are found to be in rather good agreement with experimental data. For even isotopes with shape coexistence, no adequate constraint could be identified up to now, except perhaps the charge radius. The knowledge of the intrinsic deformation allows us to interpret phenomena as charge radii staggering in term of shape coexistence. It is clear that when shape coexistence occurs the present mean-field calculation is able to interpret them, but it often fails in the prediction of the GS assignment when only the energy criterion is applied. In conclusion, the magnetic moment is found to be a valuable observable to constrain mean-field models, which still need to be improved through either new parametrizations of the interaction or extended descriptions of its functionals. Such improvements should aim at reproducing the correct energy sequence, keeping in mind that energy ordering can be also affected by beyond-mean-field corrections (e.g., through generator coordinate methods) or by dynamical effects, for example within the QRPA framework.

ACKNOWLEDGMENTS

We are grateful to P. Van Duppen, A. Barzakh, and A. Andreyev for stimulating discussions. S.G. acknowledges support as an FRS-FNRS research associate. This work was supported by the Fonds de la Recherche Scientifique (F.R.S.-FNRS) and the Fonds Wetenschappelijk Onderzoek - Vlaanderen (FWO) under the EOS Project No. O022818F.

-
- [1] B. A. Marsh, T. D. Goodacre, S. Sels, Y. Tsunoda, B. Andel *et al.*, *Nature Phys.* **14**, 1163 (2018).
 - [2] A. N. Andreyev, M. Huyse, P. Van Duppen, L. Weissman *et al.*, *Nature (London)* **405**, 430 (2000).
 - [3] P. Rakhila, D. G. Jenkins, J. Pakarinen, C. Gray-Jones *et al.*, *Phys. Rev. C* **82**, 011303(R) (2010).
 - [4] M. Siciliano, I. Zanon, A. Goasduff, P. R. John, T. R. Rodríguez *et al.*, *Phys. Rev. C* **102**, 014318 (2020).
 - [5] R. Julin, T. Grahn, J. Pakarinen, and P. Rakhila, *J. Phys. G* **43**, 024004 (2016).
 - [6] J. L. Wood and K. Heyde, *J. Phys. G* **43**, 020402 (2016).
 - [7] J. Libert, M. Girod, and J.-P. Delaroche, *Phys. Rev. C* **60**, 054301 (1999).
 - [8] M. Bender, G. F. Bertsch, and P.-H. Heenen, *Phys. Rev. C* **73**, 034322 (2006).
 - [9] K. Heyde and J. L. Wood, *Rev. Mod. Phys.* **83**, 1467 (2011).
 - [10] J. Egido, *Phys. Scripta* **91**, 073003 (2016).
 - [11] G. Neyens, *Rep. Prog. Phys.* **66**, 633 (2003).
 - [12] G. Ulm, S. K. Bhattacharjee, P. Dabkiewicz, G. Huber, H.-J. Kluge *et al.*, *Z. Phys. A* **325**, 247 (1986).
 - [13] R. Neugart, J. Billowes, M. L. Bissell, K. Blaum, B. Cheal *et al.*, *J. Phys. G, Nucl. Part. Phys.* **44**, 064002 (2017).
 - [14] N. Stone, *At. Data Nuc. Data Tab.* **90**, 75 (2005).
 - [15] S. Goriely, S. Hilaire, S. Péru, M. Martini, I. Deloncle, and F. Lechaftois, *Phys. Rev. C* **94**, 044306 (2016).
 - [16] I. Deloncle, S. Péru, and M. Martini, *Eur. Phys. J. A* **53**, 170 (2017).
 - [17] S. Péru, I. Deloncle, S. Hilaire, S. Goriely, and M. Martini, *Eur. Phys. J. A* **55**, 232 (2019).
 - [18] M. Bender, P.-H. Heenen, and P.-G. Reinhard, *Rev. Mod. Phys.* **75**, 121 (2003).
 - [19] S. Péru and M. Martini, *Eur. Phys. J. A* **50**, 88 (2014).
 - [20] A. Bohr and B. Mottelson, *Nuclear Structure*, Vol. 2 (Benjamin, New York, 1975).
 - [21] O. Prior, F. Boehm, and S. Nilsson, *Nucl. Phys. A* **110**, 257 (1968).
 - [22] I.-L. Lamm, *Nucl. Phys. A* **125**, 504 (1969).
 - [23] C. Ekström and H. Rubinsztein, *Phys. Scripta* **14**, 199 (1976).
 - [24] D. Sprung, S. Lie, M. Vallières, and P. Quentin, *Nucl. Phys. A* **326**, 37 (1979).
 - [25] L. Bonneau, N. Minkov, D. D. Duc, P. Quentin, and J. Bartel, *Phys. Rev. C* **91**, 054307 (2015).
 - [26] M. Chemtob and M. Rho, *Nucl. Phys. A* **163**, 1 (1971).
 - [27] S. Goriely, S. Hilaire, M. Girod, and S. Péru, *Phys. Rev. Lett.* **102**, 242501 (2009).
 - [28] National Nuclear Data Center, Brookhaven National Laboratory, <https://www.nndc.bnl.gov/nudat2/>, 2021.
 - [29] T. Day Goodacre, A. V. Afanasjev, A. E. Barzakh, B. A. Marsh, S. Sels *et al.*, *Phys. Rev. Lett.* **126**, 032502 (2021).
 - [30] M. Girod, J. P. Delaroche, A. Görgen, and A. Obertelli, *Phys. Lett. B* **676**, 39 (2009).
 - [31] T. R. Rodríguez, *Phys. Rev. C* **90**, 034306 (2014).
 - [32] J. M. Boillos and P. Sarriguren, *Phys. Rev. C* **91**, 034311 (2015).
 - [33] M. Martini, S. Péru, and S. Goriely, *Phys. Rev. C* **89**, 044306 (2014).
 - [34] A. Gottardo *et al.*, *Phys. Lett. B* **772**, 359 (2017).

- [35] B. Andel, A. N. Andreyev, S. Antalic, M. AlMonthery, A. Barzakh *et al.*, *Phys. Rev. C* **102**, 014319 (2020).
- [36] M. Preston, *Physics of the Nucleus*, Addison-Wesley World Student Series Edition (Addison-Wesley, Boston, 1965).
- [37] R. D. Harding, A. N. Andreyev, A. E. Barzakh, D. Atanasov, J. G. Cubiss *et al.*, *Phys. Rev. C* **102**, 024312 (2020).
- [38] G. Audi, F. Kondev, M. Wang, W. Huang, and S. Naimi, *Chin. Phys. C* **41**, 030001 (2017).
- [39] J. Sauvage, F. Ibrahim, B. Roussi re, J. Genevey, A. Gizon *et al.*, *Eur. Phys. J. A* **25**, 5 (2005).
- [40] A. Algora, E. Ganioglu, P. Sarriguren, V. Guadilla, L. M. Fraile *et al.*, *Phys. Lett. B* **819**, 136438 (2021).